SolarPACES 2022, 28th International Conference on Concentrating Solar Power and Chemical Energy Systems
Power Cycles
https://doi.org/10.52825/solarpaces.v1i.730

Published: 18 Dec. 2023

# Economic Optimization of a Thermal Solar Power Plant that Operates with a HRB Cycle by Improving the Operation Schedule

Antonio J. Subires[1] [https://orcid.org/0000-0001-8438-8636], and Antonio Rovira[1] [https://orcid.org/0000-0002-6810-3757]

[1] Universidad Nacional de Educación a Distancia (UNED), c/ Juan del Rosal, 12, 28040 Madrid, Spain

**Abstract.** In this paper, two solutions are proposed to increase the sales revenue of a pre-sized solar thermal power plant (STPP) that operates with a Hybrid Rankine Brayton cycle (HRB) by changing the reference operating parameters. In the first solution, the turbine inlet temperature value is optimized to increase the energy production. In the second solution, a new dispatch strategy that prioritizes energy production during the hours of higher sales price is additionally implemented in low solar radiation months. In the remaining months, the reference dispatch strategy that prioritizes production from energy coming directly from the solar field over energy from storage system is maintained. The incremental sales revenue of each solution proposed over the reference case is calculated considering hourly SPOT prices for a three-year period and considering hourly annual simulations for a typical year.

**Keywords:** Medium Temperature Solar Thermal Energy, STPP, B-HRB, CSP.

## 1. Introduction

The profitability obtained from the operation of a power plant can be improved by lowering costs (such as O&M costs) or by increasing revenues. The revenues can be increased in two ways: Increasing the annual energy production or increasing the average sale price per unit of energy. In the first case, operating parameters that increase either the energy production efficiency or the primary energy used are modified. In the second case, energy is generated when the sale price allows greater revenue. Not all renewable electricity production technologies can use this option to increase their incomes since they depend on the availability of the natural resource.

STPPs with thermal energy storage system (TES) can store the absorbed energy and manage when to transfer it to the power block (PB). This allows for adapting production to demand, regardless of whether demand peaks occur when there is no solar radiation. The Spanish electricity market is a pay as-cleared market in which the sale prices are determined in hourly periods through a daily auction. Therefore, it could be interesting to produce around demand peaks, especially during the demand peak after sunset. However, the most widespread management strategy in Spain prioritizes production from energy coming directly from the solar field over energy from the storage [1], [2]. Usaola [3] compares the benefits of two operational scenarios in a Spanish STPP, one of them following the real scenario, and the other following an optimized operation model around hours with higher energy sale prices. The results shown that with the Spanish subsidy policy, the benefits of the optimized operation are lower than the production operation that prioritizes energy that comes directly from the solar field. This was because the largest part of the planter venue comes from a fixed premium, not modulated by the market price. In [4] a new comparison is done considering the new subsidy

policies implemented in Spain in 2013. Although these policies are more restrictive than the previous ones, it is demonstrated that the weight of subsidies is still significant enough to prioritize an operation strategy based on electricity production from thermal energy that comes directly from the solar field. This study concludes that in order to make STPPs economically viable in Spain without subsidy policies, several measures need to be taken. These include increasing the nominal power capacity of new STPPs beyond the current 50 MW limit, enhancing the energy storage capacity, and establishing an operation strategy that aligns more closely with the demand curve, regardless of whether production occurs during non-solar radiation hours.

In this work, we have proposed two solutions that improve the profitability of a STPP in a scenario without subsidy policies. The reference case is a STPP that works with a constant turbine inlet temperature operation and a dispatch strategy that prioritizes energy that comes directly from the solar field. In Solution 1, the constant inlet temperature setting criterion of the reference case has been changed to a variable turbine inlet temperature setting criterion, keeping constant the difference between the HTF flow temperature that enters in the SSG and the turbine inlet temperature. In Solution 2, in addition to the variable turbine inlet temperature setting criterion, we have considered a new dispatch strategy that prioritizes energy production at sunset in low solar radiation months, during the hours of higher sales price. Design parameters are maintained in both cases, so no new costs are incurred.

## 2. Reference data

We have performed the calculations using MATLAB, integrating Refprop databases to obtain the properties of propane (power fluid) and air (refrigerant). We have created databases for Therminol VP1 (HTF) and molten salts (heat storage fluid) using the expressions proposed in [5,6]. The meteorological data used to calculate the annual simulations, corresponds to a database of a typical year for Sevilla provided by METEONORM. It includes the weather station coordinates, as well as values taken hourly of Direct Normal Irradiation (DNI) and dry bulb temperature. These data can be found in Table 1. The annual simulation results of the reference case have been validated using SAM. The economic analysis has been done considering databases of hourly SPOT prices (€/MWh) for the years 2017, 2018 and 2019 provided by [7].

The power plant design is the same for all the cases considered. It is a 100 MW STPP with a parabolic trough solar field located in Sevilla that operates with a propane HRB power cycle. This cycle was proposed by Rovira et al. [8] and it is a good alternative to conventional power cycles, achieving similar performance with greater simplicity. Figure 1 shows the layout of the reference HRB power cycle and its T-s diagram. The design parameters used to pre-size the different systems of the power plant are shown in Table 1. The nominal ambient conditions for the solar field have been taken at 12:00 p.m. (solar time) on June 21.

The solar field is based on parabolic trough collectors (ET-150 with Schott PTR70 receivers) in which Therminol VP-1 (HTF) transfers the thermal solar energy to the power cycle through a heat exchanger (SSG). The solar field has 264 loops. Each loop is composed of 4 Solar Collector Assemblies (SCAs) distributed in two rows. The solar multiple is 2, so in nominal conditions half of the absorbed solar power is transferred to the power cycle and half is stored. The TES is a two-tank system with a storage capacity for 12 hours of nominal PB thermal power requirement. The power cycle nominal efficiency is 39.98%. It is reached with a 0.25 compressor recirculation factor value and 14:1 compression ratio. In these conditions, the air-cooling system power consumption is 6.8 MW. Heat exchangers (Recuperator, SSG, condenser and molten salts/HTF heat exchanger) have been pre-sized calculating the UA factors. A dataset that contains all the results is included as Supplementary Material.

**Table 1**. Input parameters under design conditions.

| | | | |
|---|---|---|---|
| **1. Ambient conditions** | | **3. Storage system parameters** | |
| Dry Bulb Temperature | 25 ºC | Cold/Hot salts temperature | 285/391ºC |
| Direct Normal Irradiation | 850 W/m$^2$ | 12 h capacity | |
| **2. Solar field parameters** | | **4. Air cooling system parameters** | |
| Latitude, longitude | $\lambda(37.41º); L(-5.9º)$ | Fan isentropic efficiency | 0.8 |
| Outlet/Inlet Temperature | 396/290 ºC | Fan mechanical efficiency | 0.94 |
| **a) *Collector parameters*** | | Condenser Initial Temperature difference* | 10ºC |
| Reflective aperture area of one collector assembly | 817.5 m$^2$ | Condenser Approach temperature | 3ºC |
| | | Fan pressure ratio | 1.0028 |
| Length of one collector assembly | 150 m | **5. Power cycle parameters** | |
| Aperture width | 5.75 m | Power | 100 MW |
| Mirror reflectance | 0.92 | Condenser temperature | 35 ºC |
| Intercept factor | 0.92 | Turbine inlet temperature | 377 ºC |
| **b) *Receiver parameters*** | | Recuperator Pinch Point | 5ºC |
| Absorber tube inner diameter | 0.066 m | Turbomachinery polytropic efficiency | 0.9 |
| Absorber tube outer diameter | 0.07 m | SSG pressure drop** | 2% |
| Envelope transmittance | 0.963 | Recuperator pressure drop*** | 5% |
| Absorber absorptance | 0.96 | | |
| Mass flow rate per loop | 7.725 kg/s | | |

* It is defined as the difference between the propane condensing temperature and the refrigerant inlet temperature.
** The SSG pressure drop corresponds to the high-pressure side. The pressure is assumed to decrease linearly.
*** The recuperator pressure drop corresponds to the low-pressure side. The pressure is assumed to decrease linearly.

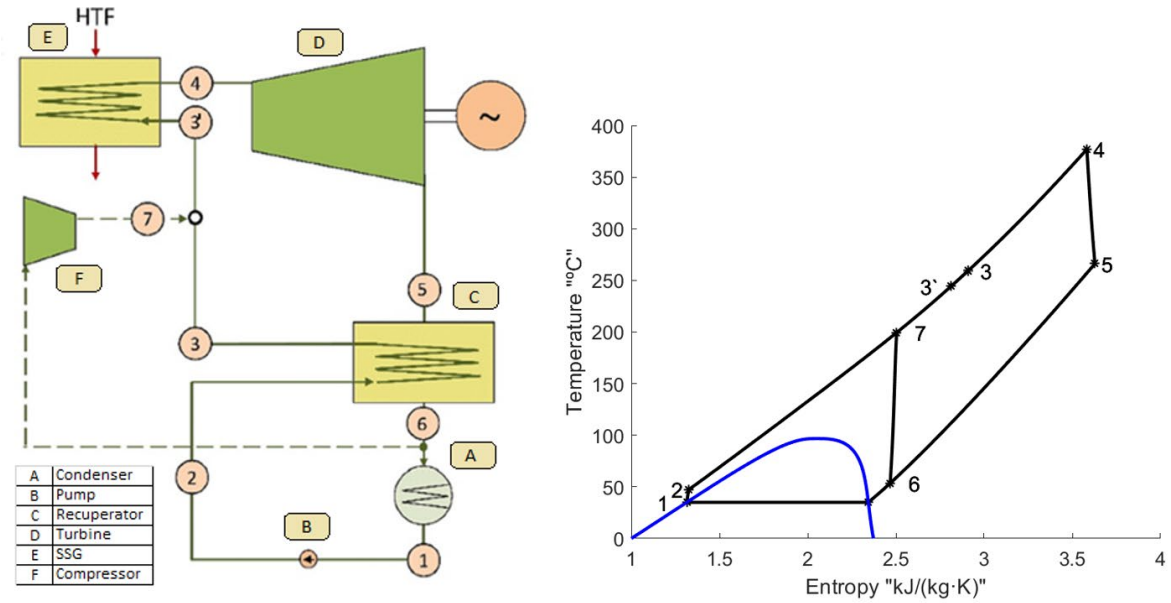


**Figure 1**. Layout (left) and T-s diagram (right) of the HRB cycle.

# 3. Methodology

## 3.1 Off-design calculation methodology

The power cycle turbomachinery off-design behaviour is characterised assuming the following criteria: **1)** The Stodola-Frügel Law describes the steam turbine operation [9]. **2)** The turbomachinery efficiency is reduced from the nominal value as the capacity moves away from the design value. Equation (1) relates the turbomachinery efficiency to its capacity. The turbomachinery capacity depends on the flow rate, the pressure, and the inlet temperature.

UA factors decrease as the mass flow rate of the fluid with the highest thermal resistance also does. Equation (2) relates the design and off-design values for UA factor and mass flow rate.

$$\eta_{tb} = \eta_{tb_{dis}} - \left|1 - \frac{\phi_{tb}}{\phi_{tb_{dis}}}\right| / 3 \ where \ \ \phi = \dot{m}\frac{\sqrt{T}}{P} \quad (1)$$

$$UA_{\ obj} = UA_{dis} \cdot \left(\frac{\dot{m}_{HTF}}{\dot{m}_{HTF_{dis}}}\right)^{0.8} \quad (2)$$

$\eta_{tb}$ is the efficiency of turbine in off-design conditions; $\eta_{tb_{dis}}$ is the efficiency of turbine in nominal conditions; $\dot{m}\ (kg/s)$ is the propane mass flow rate that enters in the turbine; $T\ (K)$ is the temperature and $P\ (Pa)$ the pressure.

$UA_{obj}\ (MW/K)$ is the overall heat transfer coefficient in off-design conditions multiplied by the total area; $UA_{dis}\ (MW/K)$ is the overall heat transfer coefficient in design conditions multiplied by the total area; $\dot{m}_{HTF}$ is the HTF mass flow rate that enters in the heat exchanger; $\dot{m}_{HTF_{dis}}$ is the design HTF mass flow rate that enters in the heat exchanger.

## 3.2 Annual simulations. General considerations

The following effects are considered in all simulations: **1)** Thermal losses of storage tanks are calculated hourly using the expressions showed in [10]. These equations are based on a dimensionless analysis performed on tanks that have the same diameter-to-height ratio as ANDASOL I tanks [11]. **2)** Row shadowing losses are assessed by the shadow factor [12]. **3)** Solar field startup thermal energy is calculated considering the hourly HTF energy state and the thermal inertia of headers and SCA components (Equation 3). The hourly HTF energy state is calculated considering the HTF volumes (*V*) of each system: loops, cold pipe headers (*c,hd*), hot pipe headers (*h,hd*) and SSG (Equation 4). It depends on the HTF density ($\rho$), the HTF enthalpy ($h$) and the number of total loops ($N_{lps}$). The energy state of headers and SCA components is calculated by Equation (5). It considers cold and hot headers thermal inertia ($mc_{c,hd}, mc_{h,hd}$) as well as loop thermal inertia ($mc_{lp}$). These experimental terms are proposed in [13]. We have considered the standard values proposed by System Advisor Model (v 2021.12.2). In Equation (5), $mc_{c,hd}$ and $mc_{h,hd}$ are multiplied by the nominal power generated ($\dot{W}_{dis}$) and the HTF temperature contained in cold and hot headers; $mc_{lp}$ is multiplied by the length of each SCA ($L_{SCA}$), the total number of total loops ($N_{lps}$), the number of SCAs per loop ($N_{SCA}$), and the average temperature of each loop ($\bar{T}_{lp}$). **4)** The PB startup is constrained by a time duration and a thermal energy fraction. The time duration constrain value is 30 min and the energy constraint value is a 20% of the thermal energy demanded by the PB during 1 hour at nominal conditions. Both conditions must be met in order to consider the startup period of the power block as completed.

$$E_{th,sf}(Wh) = 1(h) \cdot \frac{E_{th,HTF}}{3600\ (s)} + E_{th,hd+sca} \quad (3)$$

$$E_{th,HTF}(J) = N_{lps} \cdot \rho_{lp} \cdot V_{lp} \cdot h_{lp} + \rho_{c,hd} \cdot V_{c,hd} \cdot h_{c,hd} + \rho_{h,hd} \cdot V_{h,hd} \cdot h_{h,hd} + \rho_{SSG} \cdot V_{SSG} \cdot h_{SSG} \quad (4)$$

$$E_{th,hd+sca}(Wh) = \dot{W}_{dis} \cdot \left(mc_{c,hd} \cdot T_{c,hd} + mc_{h,hd} \cdot T_{h,hd}\right) + mc_{lp} \cdot N_{SCA} \cdot N_{lps} \cdot L_{SCA} \cdot \bar{T}_{lp} \quad (5)$$

The following operation conditions are considered in all cases: **1)** The HTF mass flow rate through the SSG and the outlet temperature of the solar field take the design value; **2)** Ambient temperature and inlet SSG temperature at HTF side (in the case that the TES provides thermal energy to the PB) take off-design values; **3)** Condensation temperature is fixed 10ºC above the dry bulb temperature.

## 3.3 Annual simulations. Reference case and Solution 1.

In the reference case, the turbine inlet temperature always maintains its design value. In Solution 1, the temperature difference between the HTF entering the SSG and the turbine inlet always maintains design value. Therefore, when the HTF temperature entering the SSG takes off-design values, the turbine inlet temperature is adjusted to maintain the design temperature difference between the two flows. Besides, both follow a dispatch strategy that prioritizes production from energy coming directly from the solar field with only one PB startup per day. The following premises are considered: **1)** Every day, after the startup of the solar field and before the startup of the power block (PB), the minimum energy required to be stored is calculated to ensure uninterrupted operation of the PB during daylight hours. **2)** The PB startup operation only demands energy that comes directly from the solar field. **3)** If the power absorbed by the solar field is higher than the maximum power that the cycle can demand, the power excess is derived to the storage system. **4)** If the absorbed solar power is lower, the stored energy is transferred to the PB complementing the flow that comes from the solar field. **5)** After sunset, the salts are discharged at the nominal value, so the remaining stored energy is transferred to the PB increasing the total production time.

## 3.4 Annual simulations. Solution 2

Solution 2 considers a new dispatch strategy that prioritizes the production during the time periods with higher selling prices. In the remaining hours of the day, the power plant is turned off (in case of no solar radiation) or is storing energy. The PB startup operation begin 30 minutes before the production time period, so if the solar radiation is lower than the maximum thermal energy that the PB can absorb, the TES supplies the remaining power. The turbine inlet setting criterion is the same as in Solution 1.

This new strategy is set during the six months with lower solar radiation (January, February, March, October, November, and December). The time period in which the PB generates power is a fixed daily interval of time that is recalculated monthly. To determine it, we have first calculated the average hourly SPOT prices for each month of one year. This method is applied to each one of the three years considered. We have calculated the average hourly prices for an average year after verifying that the trend of the average hourly prices coincides for the same months of each year. Then, the time period in which PB generates power is set monthly considering the highest average hourly prices for the mean year. The new dispatch strategy also considers the energy losses due to defocussing collectors when the TES is storing energy, but the PB is off. These losses can be high because the salts flow rate cannot exceed the nominal value. To reduce them, when the accumulated energy losses over a day exceed a certain value, the reference dispatch strategy that prioritizes production from energy coming directly from the solar field is set for that day, recalculating the simulation.

The next steps are considered in case that the cold salts tank is emptied during an energy storage operation: **1)** The simulation is recalculated from two days before the day the tank is emptied, extending one hour the generating power time interval. The extended time interval applies only to the day from which the simulation is recalculated. The extended hour corresponds to the hour with the highest possible average price. **2)** If the tank is emptied again on the same day, step 1) is repeated from the day before the tank was emptied. **3)** If the tank is emptied again on the same day, there are two possibilities: **3a)** If the tank is emptied the hour before the production period starts and this hour has the highest possible average price, the production time period is extended. **3b)** If none of the conditions in 3a) are met, the previous steps are repeated, extending the production interval for one more hour. This methodology simulates the operation of a real power plant in which weather conditions are known two days in advance.

In Figure 2 an example of flux chart is showed to clarify the methodology exposed: In *n* day, the cold salts tank is emptied two times. When it happens for the first time, the “x” hour

is added to the production "*h"* interval in day n-2. That corresponds with the step **1)** of the methodology. Then, the simulation is recalculated again until day n, in which the cold salts tank is emptied again. In this time, the "x" hour is added to the production "*h" interval* in day n-1. That corresponds with the step **2)** of the methodology. If the tank were to be emptied more times, another hour "y" would be added following the same steps.

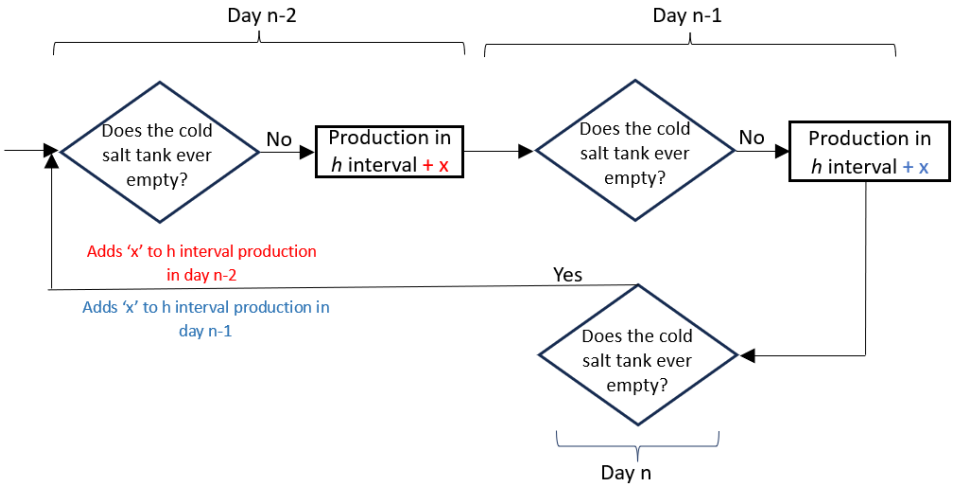


**Figure 2.** Example of flux chart.

# 4. Results

## 4.1 Hourly SPOT prices analysis.

Figure 3 and Figure 4 shows the average hourly SPOT prices for each month of the mean year. In all months there are two periods of peak prices and another two of valley prices. During low radiation months, peak price periods occur around the sunset and sunrise. Prices around sunset are higher than around sunrise. Regarding the valley price periods, one of them is around high radiation hours (usually between 12 a.m. and one or two hours before the sunset) and the other one occurs during no radiation hours (usually between 0 a.m. and one or two hours before the sunrise). This behaviour is similar during high radiation months but the difference between the mean price of the periods is lower.

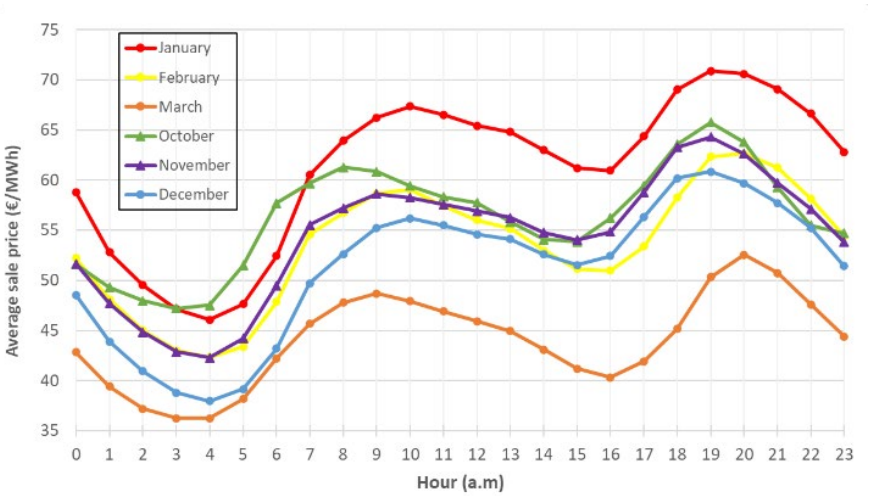


**Figure 3.** Mean hourly sale price for low radiation months.

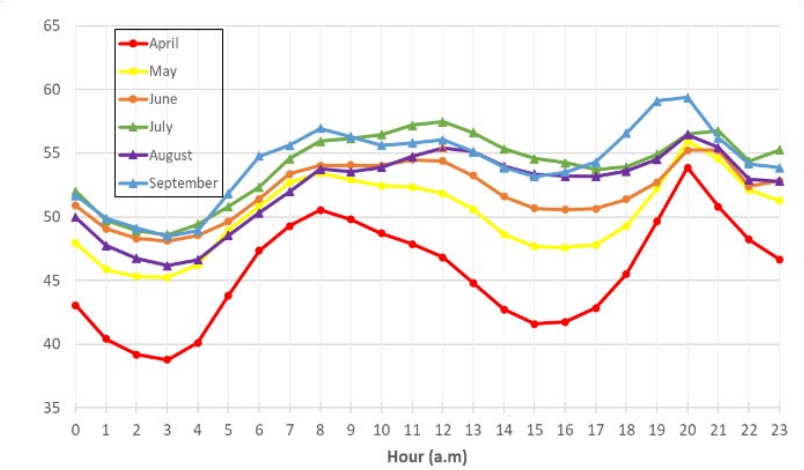


**Figure 4.** Mean hourly sale price for high radiation months.

## 4.2 Comparison between the reference case and Solution 1.

Table 2 shows the comparison between the main results of the annual simulation for the reference case and Solution 1. The thermal energy demanded by the PB ($Q_{PB,net}$) is the difference between the total energy absorbed by the solar field ($Q_{solar,abs}$) minus the sum of the solar field startup thermal energy ($Q_{start,sf}$), the PB startup thermal energy ($Q_{start,PB}$) and the thermal energy losses in the molten salt tanks ($Q_{TES,loss}$). The total net energy generated ($E_{net,PB}$) is the total energy produced by the PB ($E_{tot,PB}$) minus the energy consumed by the air-cooling system.

**Table 2**. Main results of the annual simulation for the reference case and Solution 1

| Case | Reference | Solution 1 |
|---|---|---|
| $Q_{solar,abs}$ (GWh) | 1016.6 | 1039.4 |
| $Q_{start,sf}$ (GWh) | 103.7 | |
| $Q_{start,PB}$ (GWh) | 16.9 | |
| $Q_{TES,loss}$(GWh) | 8.6 | |
| $Q_{PB,net}$ (GWh) | 887.5 | 910.2 |
| $E_{tot,PB}$(GWh) | 349.9 | 357.4 |
| $E_{net,PB}$ (GWh) | 326.2 | 332.9 |
| $Eff_{PB}$ (%) | 39.43 | 39.27 |

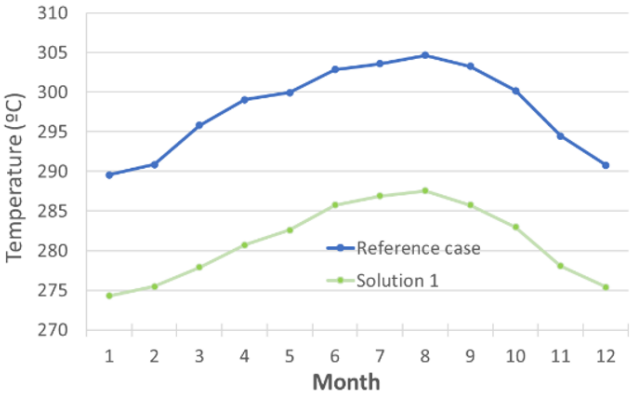


**Figure 5.** Monthly mean temperature in cold salts tank

$E_{net,PB}$ is higher in Solution 1 despite the PB efficiency ($Eff_{PB}$) is lower. It is because $Q_{solar,abs}$ is increased as result of the higher maximum solar power that can be absorbed and stored before defocussing colectors. The maximum solar power absorbed depends on cold salt tank temperature, which is lower in Solution 1. Figure 5 shows the monthly mean temperature of the cold salts tank for each case. In Solution 1, salts are discharged to the cold tank with a lower temperature in the partial and total salt discharge operations as it is shown in Table 3. For that reason, the thermal power discharged from the TES and the power generated by the PB is higher in Solution 1 than in the reference case for the same environmental conditions.

Table 4 shows the monthly net energy production and the monthly revenue for a mean year in the reference case and their respective increments in Solution 1. For the reference case, the net energy production during months with high radiation is around a 74% of the total annual production. The sales revenues take a similar value. Solution 1 achieves an increase of energy production during the months of high radiation because the losses due defocussing

collectors are high for the reference case. During these months, the thermal energy stored is usually enough to keep the production some hours after 0 a.m. (valley prices period). The hot salts tank is emptied earlier in Solution 1 so the number of production hours after 0 a.m is lower. However, more power is produced during the peak prices period after sunset. For that reason, the sales revenue increment is higher than the energy production increment. During the low radiation months, the sales revenue increment is sometimes lower than the energy increment, reaching negative values in some months. This is because less energy is produced during the two peak price periods as the PB demands more thermal power from the TES. The production during the morning peak price period is reduced as more energy must be stored before the PB startup. The production during the sunset peak price period is reduced because the hot salts tank is usually emptied just after sunset.

The annual production increment of Solution 1 over the reference case is 2.03% and the annual revenue increment is 2.29%.

**Table 3**. Hourly simulation results in two representative points for the reference case and Solution 1

| **Operation condition** | **Partial TES discharge** | | **Total TES discharge** | |
|---|---|---|---|---|
| Case | Reference | Solution 1 | Reference | Solution 1 |
| Date | February 9 at 17 a.m. | | July 25 at 22 a.m. | |
| Dry bulb temperature (ºC) | 15.1 | | 27.2 | |
| Solar thermal power (MW) | 154 | 155 | 0 | |
| Thermal power stored (MW) | -92 | -110 | -207 | -243 |
| Thermal power to cycle (MW) | 246 | 265 | 207 | 243 |
| Electrical power produced (MW) | 102 | 108 | 81 | 94 |
| Power block efficiency (%) | 41.36 | 40.93 | 39.05 | 38.88 |
| Cold salts temperature (ºC) | 290 | 281 | 304 | 288 |
| Hot salts temperature (ºC) | 390 | 389 | 392 | 391 |
| Molten salts mass flow rate factor* | -0.39 | -0.43 | -1 | -1 |
| SSG inlet HTF temperature (ºC) | 392 | 390 | 388 | 387 |
| SSG outlet HTF temperature (ºC) | 287 | 277 | 300 | 283 |
| Turbine inlet temperature (ºC) | 377 | 371 | 377 | 368 |
| *It is defined as the fraction of design molten salts mass flow rate that circulates in the non-design condition considered | | | | |

**Table 4.** Monthly results for reference case and Solution 1

| | | *Jan.* | *Feb.* | *Mar.* | *Apr.* | *May* | *June* | *July* | *Aug.* | *Sep.* | *Oct.* | *Nov.* | *Dec.* |
|---|---|---|---|---|---|---|---|---|---|---|---|---|---|
| **Reference case** | *Net Energy (GWh)* | 9.8 | 11.7 | 25.3 | 29.4 | 37.6 | 45.1 | 53 | 45.7 | 30.7 | 18.5 | 12.3 | 7 |
| | *Sales Revenue (M€)* | 0.64 | 0.63 | 1.12 | 1.36 | 1.92 | 2.34 | 2.87 | 2.42 | 1.7 | 1.06 | 0.67 | 0.38 |
| **Solution 1** | *Net Energy Incr. (%)* | 0.12 | 0.34 | -0.08 | 1.2 | 2.62 | 2.15 | 4.93 | 2.44 | 1.64 | 0.29 | 0.01 | 0.17 |
| | *Sales Revenue Incr. (%)* | -0.02 | 0.28 | 0.28 | 1.78 | 2.95 | 2.33 | 4.9 | 2.86 | 2.09 | 0.48 | -0.06 | 0.66 |

Figure 6 and Figure 7 show different hourly parameters of the simulation for the reference case and Solution 1 on May 25th. Figure 1 shows the hourly gross power of each case along with the corresponding hourly price curve. The power produced for the reference case decreases as the proportion of energy from storage increases relative to solar field energy. This occurs at 11 a.m. and 7 p.m. (combined contribution of energy from the solar field and storage) and from 8 p.m. onwards (energy from storage only). For Solution 1, the power decrement is not as significant when the energy comes from storage. As a result, Solution 1 generates higher power during the peak price hours at sunset (between 7 p.m. and 11 p.m.).

Figure 7 shows the percentage of filling in the hot salts tank and the temperature of the cold tank for the reference case and Solution 1. The percentage of filling in the hot tank for the reference case is higher than that of Solution 1, even though both tanks were initially empty at 8 a.m.. The difference in filling between the two cases increases between 8 a.m. and 12 p.m., when the salt flow rate is below the limit value. As a result, since the temperature of the cold tank is lower in Solution 1 compared to the reference case, a lower flow rate is required to store the same amount of energy. From 12 p.m. to 7 p.m., both cases reach the nominal value of salt flow rate, resulting in the storage of more energy in Solution 1. Starting from 8 p.m., the salts are discharged from the hot tank at the nominal value. Since Solution 1 achieves a lower discharge temperature to the cold tank, the thermal energy transmitted to the power block is higher than in the reference case.

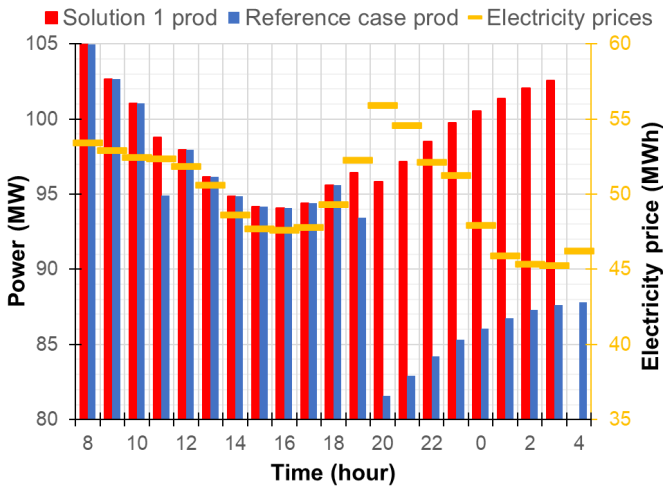


**Figure 6.** Spot prices and hourly gross power production for the reference case and Solution 1 on May 25th

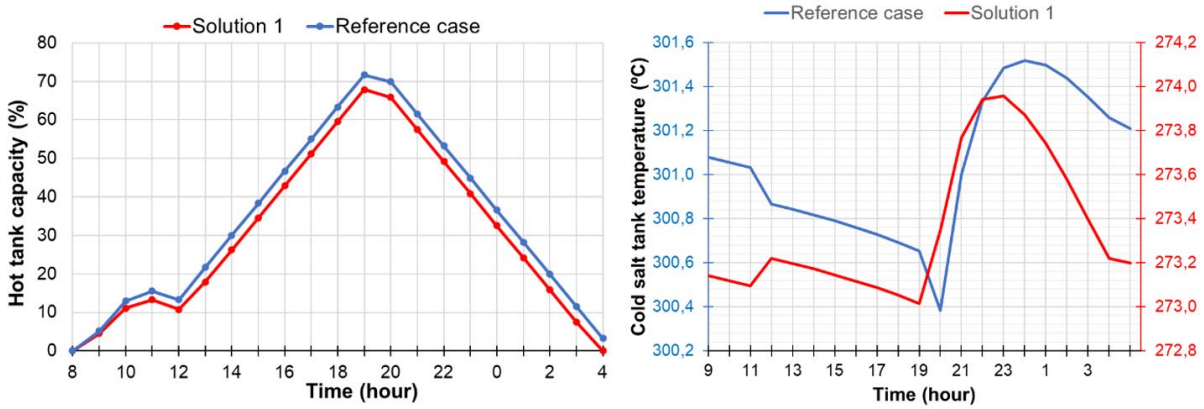


**Figure 7.** Percentage of hot salts tank filling (left) and temperature of the cold tank (right) for the reference case and Solution 1.

## 4.3 Comparison between Solution 1 and Solution 2

The production time interval is set around the peak prices period at sunset. Figure 8 shows the annual revenues increment of Solution 2 over Solution 1 depending on the production time period duration and depending on the limit value of daily energy losses due to defocusing collectors. This limit value is assessed as a fraction of the daily solar energy absorbed. Table 5 shows the hourly distribution of the interval depending on the interval duration and the month considered. In all the cases, the annual revenues increment decreases quickly when the energy limit value is higher than 15%. It is because the average sale price increment does not compensate the increase in solar energy losses. Although the 4 hours

interval is the option that most increases the average sale price, the 5 hours period interval is the option that most increases the annual revenues. It is because the 4 hours interval case implies a higher annual number of startup PB operations. Consequently, less thermal energy is available to produce power. The selected option is the 5 hours interval with a limit value of 10%. The annual revenues increment of this option is 1.67%. The annual energy production decrement is 0.09%.

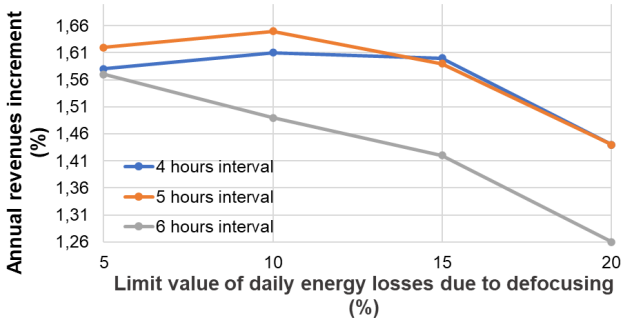


**Figure 8.** Annual revenues increment for different values of time intervals and daily energy losses limit in Solution 2

**Table 5.** Production hourly distribution

| | | Time interval duration | | |
|---|---|---|---|---|
| | | 4 h | 5 h | 6 h |
| Time (hour) for each month | Jan./Feb. | 18,19,20,21 | 18,19,20, 21,22 | 17,18,19, 20,21,22 |
| | March | 19,20,21,22 | | 18,19,20, 21,22,23 |
| | Oct. | 17,18,19,20 | 17,18,19 20,21 | 16,17,18, 19,20,21 |
| | Nov./Dec. | 18,19,20,21 | | 17,18,19, 20,21,22 |

Figure 9, Figure 10 and Figure 11 compare the distribution of the production hours between Solution 1 and Solution 2 for January, February, and March. The distribution for October, November and December follows similar trends. The results have been included as supplementary material. The yellow lines represent the spot prices. The blue and red bars show the total distribution of production hours for Solution 1 and Solution 2 respectively. The grey bars show the number of hours in which the new dispatch strategy of Solution 2 has been applied.

The production distribution in Solution 1 is mainly concentrated in the valley price period between 12 a.m. and sunset. Regarding Solution 2, the production distribution is concentrated in the production interval set for the new dispatch strategy (6 p.m. to 22 p.m.). In January, the new strategy is set all the days and the production interval has been extended only for one hour three times. In February, the limit value of loss energy is achieved in some days, so the reference dispatch strategy has been set on these days. However, unlike Solution 1, the production hours on these days are homogeneously distributed from sunrise to sunset price peak periods. It happens because the hot salt tank is not empty when solar field startup operation finishes. The result of adding the production hours of the two strategies in Solution 2 is a production concentrated in the peak price interval at sunset and distributed homogeneously during the remaining production hours. In March, the production distribution in Solution 2 follows a similar trend but with a lower concentration in the peak price interval at sunset. In Solution 2, late night production is not allowed since it corresponds to the lowest price time interval of the day.

Table 6 shows the monthly net energy production and the monthly revenues for a mean year in Solution 1 and their respective increments in Solution 2. The net energy increment in the months in which the new strategy is set, is positive in some cases and negative in others. This is because at the beginning and end of each month the hot salts tank is not empty. For the same reason, there is a net energy increment in April even though the new dispatch strategy has not been applied this month. The sales revenue is increased in all the months considered regardless of the net energy increment value.

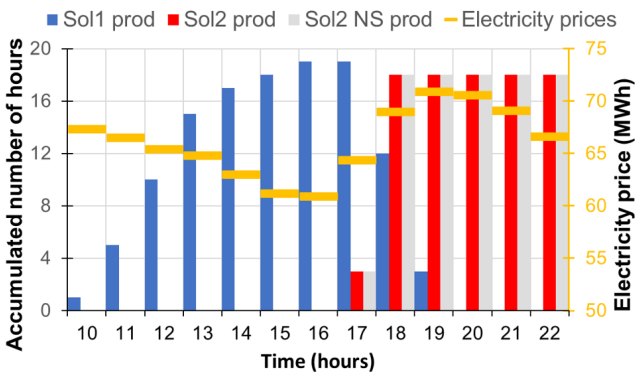


**Figure 9.** Production hourly frequency comparison in January

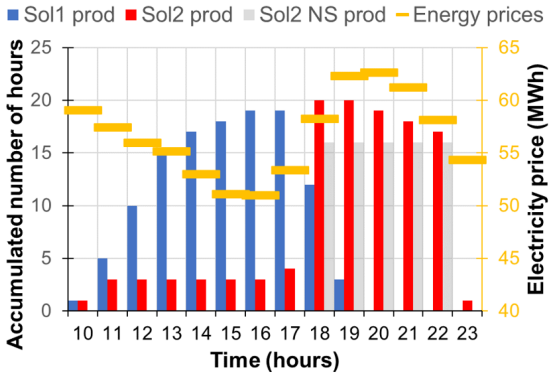


**Figure 10.** Production hourly frequency comparison in February

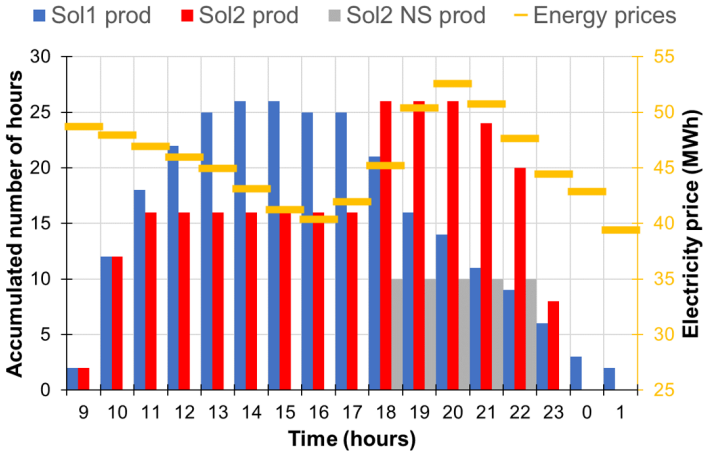


**Figure 11.** Production hourly frequency comparison in March

**Table 6.** Monthly results for Solution 1 and Solution 2

| | | *Jan.* | *Feb.* | *Mar.* | *Apr.* | *May* | *June* | *July* | *Aug.* | *Sep.* | *Oct.* | *Nov.* | *Dec.* |
|---|---|---|---|---|---|---|---|---|---|---|---|---|---|
| **Solution 1** | *Net Energy (GWh)* | 9.8 | 11.8 | 25.3 | 29.7 | 38.5 | 46.1 | 55.6 | 46.8 | 31.2 | 18.6 | 12.3 | 7 |
| | *Sales Revenue (M€)* | 0.64 | 0.63 | 1.12 | 1.38 | 1.98 | 2.4 | 3 | 2.49 | 1.73 | 1.06 | 0.67 | 0.39 |
| **Solution 2** | *Net Energy Incr. (%)* | -2.5 | 1.75 | -1.81 | 1.39 | 0 | 0 | 0 | 0 | 0 | -1.37 | -3.3 | 6.5 |
| | *Sales Revenue Incr. (%)* | 6.06 | 12.2 | 1.86 | 1.03 | 0 | 0 | 0 | 0 | 0 | 2.09 | 8.15 | 16.6 |

## 5. Conclusions

In this work, two solutions that change the operating conditions of a pre-sized STTP and increase the annual sales revenue have been proposed. Solution 1 considers a variable turbine inlet temperature setting criterion that improves the annual sales revenue by increasing the annual energy production. The greatest increment is achieved in higher solar radiation months (April to September). Solution 2 also considers a new dispatch strategy that concentrates energy production during the time interval with the highest average hourly selling price. This interval is recalculated monthly. This new strategy is considered in the lower solar radiation months (October to March) and is set only on the days in which energy losses due defocussing collectors do not exceed 10% of the daily solar energy absorbed. This strategy improves the annual results increasing the average sale price per unit of energy even though the annual energy production decreases.

Solution 2 annual sales revenue increment is around 4% over the reference case. 2.3% of the increment is due to the variable turbine inlet temperature setting criterion and 1.7% is

due to the new strategy of production during the time period with the highest hourly price. This last operation criterion is more effective although the annual revenue increment is lower since the months in which it is set represent only 26% of the annual absorbed solar energy. This dispatch strategy could be studied and implemented in all the STPPs with a TES that have been pre-sized considering the days with the highest radiation of the year. This could also reduce the large difference in hourly prices between peak and valley price periods during low radiation months.

The two solutions proposed do not increase the costs, so the profitability is higher than the sales revenue. For further work, a full economic analysis should be carried out to evaluate it.

## Data availability statement

The main sizing results of the reference STPP, the comparison of the production hours distribution between Solution 1 and Solution 2 for October, November and December, and the hourly net energy production for each month in the three cases are shown in http://dx.doi.org/10.17632/mxjzzj64k2.1.

## Author contributions

**Antonio J. Subires:** Conceptualization, Software, Writing-Original Draft, Writing-Review & Editing, Methodology, Investigation.
**Antonio Rovira:** Conceptualization, Supervision, Writing-Review & Editing, Funding acquisition, Project administration.

## Competing interests

The authors declare no competing interests that could influence the work reported on this paper.

## Fundings

Grant PID2019-110283RB-C31 and PRE2020-094353 funded by MCIN/AEI/ 10.13039/501100011033, by “ESF Investing in your future” and, as appropriate, by “ERDF A way of making Europe”, by the “European Union” or by the “European Union NextGenerationEU/PRTR”.

## References

1. Red Eléctrica de España, “redOS.” Red Eléctrica de España, Mar. 29, 2023. Accessed: Jun. 06, 2023. [Online]. Available: https://www.ree.es/en/activities/operation-of-the-electricity-system/redos-app-system-operator
2. Souza, P. Del Río, and C. P. Kiefer, “MUSTEC Working Document Issue 2 | Representative CSP Case Studies and Assessment of the Pros and Cons Lessons learned from the past,” 2020. Accessed: Jun. 06, 2023. [Online]. Available: https://mustec.eu/sites/default/files/reports/MUSTEC%20Working%20Document_Issue%202.pdf
3. J. Usaola, “Operation of concentrating solar power plants with storage in spot electricity markets,” *IET Renewable Power Generation*, vol. 6, no. 1, pp. 59–66, Jan. 2012, doi: 10.1049/iet-rpg.2011.0178.

4. G. San Miguel and B. Corona, “Economic viability of concentrated solar power under different regulatory frameworks in Spain,” *Renewable and Sustainable Energy Reviews*, vol. 91, pp. 205–218, Aug. 2018, doi: 10.1016/j.rser.2018.03.017.
5. Solutia, “Therminol VP-1. 12ºC to 400ºC,” 1999.
6. R. Ferri, A. Cammi, and D. Mazzei, “Molten salt mixture properties in RELAP5 code for thermodynamic solar applications,” *International Journal of Thermal Sciences*, vol. 47, no. 12, pp. 1676–1687, Dec. 2008, doi: 10.1016/j.ijthermalsci.2008.01.007.
7. “https://www.omie.es/es/spot-hoy.”
8. Rovira, M. Muñoz, C. Sánchez, and J. M. Martínez-Val, “Proposal and study of a balanced hybrid Rankine-Brayton cycle for low-to-moderate temperature solar power plants,” *Energy*, vol. 89, pp. 305–317, Sep. 2015, doi: 10.1016/j.energy.2015.05.128.
9. Rovira, R. Abbas, C. Sánchez, and M. Muñoz, “Proposal and analysis of an integrated solar combined cycle with partial recuperation,” *Energy*, vol. 198, May 2020, doi: 10.1016/j.energy.2020.117379.
10. Rovira, M. J. Montes, M. Valdes, and J. M. Martínez-Val, “Energy management in solar thermal power plants with double thermal storage system and subdivided solar field,” *Appl Energy*, vol. 88, no. 11, pp. 4055–4066, 2011, doi: 10.1016/j.apenergy.2011.04.036.
11. S. Relloso and E. Delgado, *Experience with molten salt thermal storage in a commercial parabolic trough plant. Andasol-1 comissioning and operation*. In: Proc of 15th int SolarPACES symposium on solar thermal concentrating technology, Berlin,Germany, 2009.
12. M. Montes, “Análisis y propuestas de sistemas solares de alta exergía que emplean agua como fluido calorífero,” Univ. Politécnica de Madrid, Madrid, 2008.
13. M. J. Wagner and P. Gilman, “Technical Manual for the SAM Physical Trough Model,” 2011. [Online]. Available: http://www.osti.gov/bridge